pyrone-side monoadduct was found.

Prior to the present work, it has been reported that irradiation of a solution of native DNA and psoralen resulted in a higher yield of pyrone adducts than furan adducts.[28] These conclusions were based on a nonquantitative, indirect assay in which only some of the adducts were isolated, and those that were isolated did not receive complete structural characterization. This interpretation agreed with theoretical predictions of the relative reactivities of the furan and pyrone double bonds of psoralens.[25,29] Our results with four different psoralens (TMP, HMT, 8-MOP, and Pso), however, reveal that the predominant event is photoaddition at the 4',5' furan double bond. Our conclusion is based on quantitative assays that involve isolation and complete structural characterization of all mono- and diadducts.

In previous work we have shown that the two diastereomeric furan-side psoralen–thymidine monoadducts are formed in unequal amounts. This is most pronounced in the case of 8-MOP, Pso, and HMT, where approximately a 2:1 preference was found. With TMP, the two diasteromers are formed in roughly equal amounts. If one assumes equal conversion rates for the two diastereomeric furan-side precursor monoadducts to the diastereomeric diadducts, then it would follow that a short-range sequence specificity exists for the interaction of the psoralen with double-stranded DNA. This specificity would result from a preference by the psoralen for intercalation on top of or underneath a given base pair (5'-TpX or 5'-XpT sequence).

The overall efficiency of the psoralen–nucleic acid photoreaction is dependent upon a number of interrelated factors such as drug solubility, efficiency of noncovalent binding to the nucleic acid, and quantum yields for the photocycloaddition and photodegradation reactions. A fuller understanding of these various parameters is necessary if a program of rational drug design is to be successfully applied to the development of psoralens with enhanced nucleic acid binding and cross-linking efficiencies. The methodology described in this study allows for the quantification of the mono- and diadducts formed in the psoralen–nucleic acid photoreaction. An analysis of the adducts obtained with a series of psoralens having systematic structural variations could provide structure–activity information useful in designing functionally specific psoralens. Such a study is now in progress.

Acknowledgment. This work was supported in part by the Division of Biomedical and Environmental Research (DOE) and the National Institute of General Medical Sciences, DHHW GM 25151. K.S. was supported by the Biomedical Mass Spectrometry Resource, University of California, San Francisco, CA. NMR studies were carried out at the University of California, Davis, NMR facility, under the auspices of NSF Grant CHE 79-04832 and at Stanford University under the auspices of NIH RR00711. Mass spectrometry studies were carried out at the University of California, San Francisco, Biomedical Mass Spectrometry Resource, supported by NIH Grant RR 00719, Dr. A. L. Burlingame, Director.

Registry No. 1, 66-97-7; **2**, 3902-71-4; **3**, 298-81-7; **4**, 62442-59-5; **6**, 83380-30-7; **6'**, 83435-11-4; **7**, 83380-31-8; **8**, 83380-32-9; **8'**, 83435-12-5; **9**, 83380-33-0; **10**, 83380-34-1; **10'**, 83435-13-6; **11**, 83380-35-2; Pso-F32 (isomer 1), 83435-14-7; Pso-F32 (isomer 2), 83380-36-3; Pso-F38A (isomer 1), 83380-37-4; Pso-F38A (isomer 2), 83435-15-8; Pso-F38A di(Me_3Si) (isomer 1), 83380-38-5; Pso-F38A di(Me_3Si) (isomer 2), 83435-16-9; Pso-F38B (isomer 1), 83380-39-6; Pso-F38B (isomer 2), 83435-17-0; Pso-F38B tetra(Me_3Si) (isomer 1), 83398-66-7; Pso-F38B tetra(Me_3Si) (isomer 2), 83461-44-3; Pso-F41 (isomer 1), 83380-40-9; Pso-F41 (isomer 2), 83435-18-1; 8-MOP-F33 hexa(Me_2Si) (isomer 1), 83380-41-0; 8-MOP-F33 hexa(Me_3Si) (isomer 2), 83435-19-2; 8-MOP-F36 (isomer 1), 83380-42-1; 8-MOP-F36 (isomer 2), 83435-20-5; 8-MOP-F37 (isomer 1), 80603-65-2; 8-MOP-F37 (isomer 2), 80656-97-9; 8-MOP-F42 (isomer 1), 83435-21-6; 8-MOP-F42 (isomer 2), 80603-69-6; TMP-F35 hexa(Me_3Si) (isomer 1), 83380-43-2; TMP-F35 hexa(Me_3Si) (isomer 2), 83461-45-4; TMP-F47 (isomer 1), 83380-44-3; TMP-F47 (isomer 2), 83435-22-7; TMP-F49 (isomer 1), 80603-66-3; TMP-F49 (isomer 2), 80657-61-0; TMP-F52 (isomer 1), 83435-23-8; TMP-F52 (isomer 2), 80659-95-6; HMT-F31 hepta(Me_3Si) (isomer 1), 83380-45-4; HMT-F31 hepta(Me_3Si) (isomer 2), 83435-24-9; HMT-F43 (isomer 1), 77340-93-3; HMT-F43 (isomer 2), 77268-07-6; HMT-F40A (isomer 1), 77268-05-4; HMT-F40A (isomer 2), 77340-92-2; HMT-F48 (isomer 1), 83380-46-5; HMT-F48 (isomer 2), 83435-25-0; poly(dA-dT)·poly(dA-dT), 26966-61-0.

Supplementary Material Available: A listing of high-resolution mass spectral data for aglycon derivatives of psoralen diadduct (1 page). Ordering information is given on any current masthead page.

(28) DallÃcqua, F.; Magno, S. M.; Zambon, F.; Rodighiero, G. *Photochem. Photobiol.* **1979**, *29*, 489.
(29) Mantulin, M. W.; Song, P. S. *J. Am. Chem. Soc.* **1973**, *95*, 5122.

Epimerization of Aldoses by Molybdate Involving a Novel Rearrangement of the Carbon Skeleton

Michael L. Hayes, Nicholas J. Pennings, Anthony S. Serianni, and Robert Barker*

Contribution from the Section of Biochemistry, Molecular and Cell Biology, Division of Biological Sciences, Cornell University, Ithaca, New York 14853. *Received March 19, 1982*

Abstract: The molybdate-catalyzed C-2 epimerization of aldoses has been investigated by using ^{13}C- and ^{2}H-enriched compounds and 75-MHz ^{13}C NMR spectroscopy. The epimerization product of D-[1-^{13}C]mannose was exclusively D-[2-^{13}C]glucose, demonstrating that the reaction involves a 1,2 shift of the carbon skeleton resulting in inversion of configuration at C-2. All of the aldotetroses, aldopentoses, and aldohexoses examined reacted similarly, producing equilibrium mixtures of the starting [1-^{13}C]aldose and the 2-epimeric 2-^{13}C product. Reaction of D-[1-^{13}C,^{2}H]mannose and D-[1,3-^{13}C,3-^{2}H]mannose in H_2O and D-mannose in $^{2}H_2O$ demonstrated that the epimerization occurs without C-3 transposition or C–H bond breaking. Studies with aldose analogues including mannitol, 3-deoxy-D-*arabino*-hexose, 4-deoxy-D-*lyxo*-hexose, lactose, and 4,6-*O*-ethylidene-D-glucose suggest that the reactive molybdate complex involves the carbonyl oxygen and three hydroxylic oxygens of the aldehyde form of aldoses. The rates of reaction are influenced by the ability of the ring forms of the starting aldose to form stable unreactive molybdate complexes. Slower secondary reactions involving the simultaneous inversion of configuration of C-2 and C-3 occur without carbon skeletal rearrangement.

In an extensive series of reports, Bilik and his co-workers have shown that in mildly acidic solutions of molybdate, aldotetroses,[1] aldopentoses,[2,3] and aldohexoses[4,5] epimerize at C-2 with the formation of a thermodynamic equilibrium mixture of the two

0002-7863/82/1504-6764$01.25/0

epimers. Generally, the reaction proceeds without the production of ketoses, and only minor amounts of secondary products are formed. On the basis of experiments with D-[1-^{3}H]glucose that gave D-[2-^{3}H]mannose as the major product (along with starting hexose), it was proposed that the reaction occurs by hydrogen exchange between C-1 and C-2 of the cyclic sugar with inversion of configuration at both carbons.[4]

The reaction is useful for the synthesis of relatively rare sugars from their C-2 epimers, e.g., L-ribose from L-arabinose[2] and 6-deoxy-L-talose from L-fucose,[6] as well as being of theoretical importance.

We have been interested in the synthesis of carbohydrates enriched with stable isotopes for use in conformational[7] and molecular dynamic studies[8] and for the study of chemical and biochemical reaction mechanisms.[9] The Kiliani cyanohydrin reaction has been modified to prepare two C-2 epimeric [1-^{13}C]aldoses in high yield from cyanide and a parent aldose.[10,11] This method was also extended to prepare ^{2}H-, ^{17}O-, and ^{18}O-enriched compounds.[12,13] However, in some cases, only one of the C-2 epimeric products is utilized, and a means of converting the unutilized compound to its C-2 epimer is highly desirable. The epimerization catalyzed by molybdate appeared ideal for this purpose. We find, however, that treatment of D-[1-^{13}C]mannose with molybdate results in a stereospecific rearrangement of the carbon skeleton with the exclusive formation of D-[2-^{13}C]glucose. This unanticipated result prompted the present study utilizing ^{13}C- and ^{2}H-enriched carbohydrates to examine the reaction characteristics and mechanism.

Experimental Section

Materials. Molybdic acid (85%) was obtained from the Fisher Chemical Co. Dioxobis(2,4-pentanedionato-*O,O'*)molybdenum(VI), $MoO_2(acac)_2$, was purchased from Alfa Products. K^{13}CN was supplied by the Los Alamos Scientific Laboratory, University of California, Los Alamos, NM, with 90.7 atom % enrichment and 99.6% purity. *N,O*-Bis(trimethylsilyl)trifluoroacetamide (BSTFA) with 1% trimethylchlorosilane (TMCS) was obtained from Pierce Chemical Co. ^{13}C- and ^{2}H-enriched carbohydrates were prepared as described previously.[10-12] 3-Deoxy-D-[1-^{13}C]*arabino*-hexose, 4-deoxy-D-*lyxo*-hexose, and 4-deoxy-4-fluoro-D-[1-^{13}C]glucose were kindly provided by Dr. James R. Rasmussen, Department of Chemistry, Cornell University.

General Epimerization Reaction. (1) Aqueous Solvent. A solution of aldose (0.1 M) and molybdic acid (85%) (5 mM), pH 4.5, was incubated at 90 °C for 2–13 h. The mixture was treated batchwise and separately with excess Dowex 50-X8 (H^+) and Dowex 1-X2 (HCO_3^-) prior to ^{13}C NMR spectroscopy or fractionation by column chromatography on Dowex 50-X8 (200–400 mesh) (Ca^{2+}) with H_2O as eluent.[14] Fractions (10 mL) were collected at 0.5 mL/min and were assayed for aldose with phenol–sulfuric acid.[15] Fractions containing sugar were pooled and concentrated at 35 °C in vacuo to dryness prior to ^{13}C NMR or GLC analysis.

(2) Aprotic Solvent. To a solution of aldose (0.1–0.5 M) in dimethylformamide (DMF) was added 0.05 equiv of $MoO_2(acac)_2$.[16] The solution was incubated at 50 °C for 5–24 h. After cooling the solution to 5 °C, two volumes of H_2O were added and the mixture was extracted twice with two volumes of CH_2Cl_2. The aqueous layer was deionized as described above. This method is preferred for the epimerization of pentoses and tetroses since the formation of secondary products is suppressed.[16]

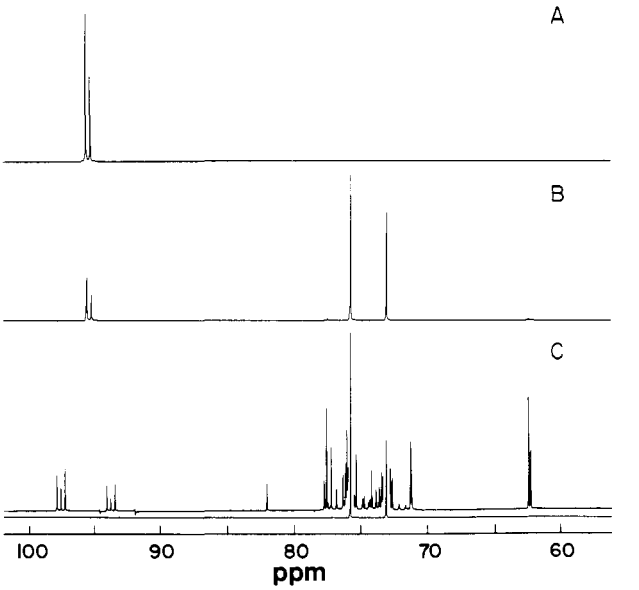

Figure 1. 75-MHz ^{13}C NMR spectra of the reaction of D-[1-^{13}C]-mannose (0.1 M) with molybdic acid (85%) (5 mM) at 90 °C for 4 h. (A) Starting material. (B) Reaction mixture showing two new enriched-carbon resonances. Only enriched carbons are visible in spectra A and B. (C) Isolated D-[2-^{13}C]glucose (lower spectrum) and the expanded spectrum (80×) showing the unenriched carbons and the splitting caused by ^{13}C at C-2.

Table I. Comparison of Calculated and Observed Equilibria between 2-Epimeric Aldoses

A ⇌ B equilibrium	[A]/[B] calcd[a]	[A]/[B] obsd
Glc ⇌ Man	2.3	2.5
Gal ⇌ Tal	6.1	4.0
All ⇌ Alt	1.9	1.5
Xyl ⇌ Lyx	2.0	1.6
Ara ⇌ Rib	2.2	2.0

[a] Calculated from $\Delta G^{\circ\prime}$ values given by Angyal.[19]

Instrumentation. Carbon-13 NMR spectra were obtained at 75 MHz with a Bruker WM-300 superconducting FT spectrometer equipped with quadrature detection. Routine spectra were obtained at 35 °C with 16 K real data points, with the spectrometer locked to the resonance of ^2H_2O in the sample. For kinetic experiments, the sample temperature (90 ± 1 °C) was measured in situ with a Fluke 2190A digital thermometer equipped with a copper–constantan thermocouple and a standard solution of identical composition with the sample but without isotopic enrichment. Spectra were obtained with 80° pulse angles, 25-s delay times, 5000-Hz spectral widths, and 8 K real data points. Areas were determined by computer integration. Chemical shifts (±0.15 ppm) are given relative to internal Me_4Si by setting spectral parameters to give the anomeric resonance of β-D-[1-^{13}C]glucopyranose at 97.4 ppm.[17]

Gas–liquid chromatography (GLC) was performed on a Varian 2100 gas chromatograph equipped with flame-ionization detection. A 2 m × 2 mm i.d. glass column packed with 3% OV-17 on HP-Chromosorb W-AW (100–120 mesh) was used with a temperature program from 100 to 230 °C at 4 °C/min. Per(trimethylsilyl) derivatives of aldoses were prepared by adding aqueous samples (6 μL) to 150 μL of dry pyridine followed by 150 μL of BSTFA containing 1% TMCS and incubating at 60 °C for 25 min.

(1) Bilik, V.; Stancovik, L. *Chem. Zvesti* **1973**, *27*, 544–546.
(2) Bilik, V.; Caplovic, J. *Chem. Zvesti* **1973**, *27*, 547–550.
(3) Bilik, V.; Petrus, L.; Farkas, V. *Collect. Czech. Chem. Commun.* **1978**, *43*, 1163–1166.
(4) Bilik, V.; Petrus, L.; Farkas, V. *Chem. Zvesti* **1975**, *29*, 690–696.
(5) Bilik, V.; Petrus, L.; Zemek, J. *Chem. Zvesti* **1978**, *32*, 242–251.
(6) Bilik, V.; Petrus, L.; Stancovic, L.; Linek, K. *Chem. Zvesti* **1978**, *32*, 372–377.
(7) Rosevear, P. R.; Nunez, H. A.; Barker, R. *Biochemistry* **1982**, *21*, 1421–1431.
(8) Hayes, M. L.; Serianni, A. S.; Barker, R. *Carbohydr. Res.* **1982**, *100*, 87–101.
(9) Serianni, A. S.; Nunez, H. A.; Barker, R. *J. Org. Chem.* **1980**, *45*, 3329–3341.
(10) Serianni, A. S.; Nunez, H. A.; Barker, R. *Carbohydr. Res.* **1979**, *72*, 71–78.
(11) Serianni, A. S.; Clark, E. L.; Barker, R. *Carbohydr. Res.* **1979**, *72*, 79–91.
(12) Serianni, A. S.; Barker, R. *Can. J. Chem.* **1979**, *57*, 3160–3167.
(13) Serianni, A. S.; Clark, E. L.; Barker, R. *Methods Enzymol.* **1982**, *89*, 79–83.
(14) Angyal, S. J.; Bethell, G. S.; Beveridge, R. J. *Carbohydr. Res.* **1979**, *73*, 9–18.
(15) Dubois, M.; Gilles, K. A.; Hamilton, J. K.; Rebers, P. A.; Smith, F. *Anal. Chem.* **1956**, *28*, 350–356.
(16) Abe, Y.; Takizawa, T.; Kunieda, T. *Chem. Pharm. Bull.* **1980**, *28*, 1324–1326.
(17) Walker, T. E.; London, R. E.; Whaley, T. W.; Barker, R.; Matwiyoff, N. A. *J. Am. Chem. Soc.* **1976**, *98*, 5807–5813.

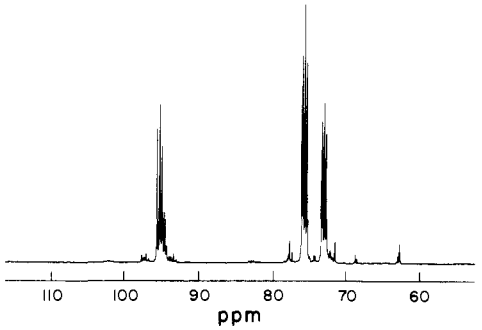

Figure 2. 75-MHz ^{13}C NMR spectrum of the reaction mixture obtained by treatment of D-[1-^{13}C,^{2}H]mannose (0.1 M) with molybdate (0.01 M) at 90 °C for 4 h. Resonances of ^{13}C-enriched carbons appear as triplets due to one-bond coupling to ^{2}H. The multiplets appearing between 72 and 77 ppm are characteristic of the product D-[2-^{13}C,^{2}H]glucose. A small amount of D-[2-^{13}C]glucose is visible as the downfield resonances in the glucose multiplets. This material is the epimerization product of the small amount of D-[1-^{13}C]mannose in the starting material, which is clearly visible in a 22.5-MHz NMR spectrum of the same mixture (data not shown).

Results and Discussion

C-2 Epimerization of D-[1-^{13}C]Aldoses. The ^{13}C NMR spectrum of D-[1-^{13}C]mannose is shown in Figure 1A. When treated with molybdate as described by Bilik[18] (90 °C, 4 h), two new resonances appeared at 75.7 and 73.0 ppm (Figure 1B). These resonances correspond in position and relative intensity to those for C-2 of β- and α-D-glucopyranose, respectively.[17] Chromatography of the reaction mixture on a Dowex 50-X8 (Ca^{2+}) column gave a column profile characteristic of a mixture of glucose and mannose, identifications that were confirmed by GLC analysis. The ^{13}C NMR spectrum of the first peak is shown in Figure 1C. All chemical shifts of the unenriched carbons correspond to those for D-glucose, and the C-1 and C-3 resonances show large one-bond C–C coupling constants (46.3 and 38.4 Hz, respectively), as expected for a 2-^{13}C-enriched aldose.[8,17] Other ^{13}C-enriched aldoses gave similar results: D-[1-^{13}C]talose, D-[1-^{13}C]galactose, D-[1-^{13}C]glucose, 6-deoxy-L-[1-^{13}C]talose, 6-deoxy-L-[2-^{13}C]talose, D-[1-^{13}C]xylose, and D-[1-^{13}C]arabinose gave D-[2-^{13}C]galactose, D-[2-^{13}C]talose, D-[2-^{13}C]mannose, L-[2-^{13}C]fucose, L-[1-^{13}C]-fucose, D-[2-^{13}C]lyxose, and D-[2-^{13}C]ribose, respectively. The reactions are reversible, and equilibria are determined by the relative thermodynamic stabilities of the interconverting aldoses (Table I). With extended reaction times, minor amounts of aldoses are formed that are C-3 epimers of the original reactant and primary product.

Bilik et al.[4] have shown that H-1 and H-2 exchange during epimerization, with D-[1-^{3}H]mannose converting to D-[2-^{3}H]-glucose. They proposed that epimerization occurs by a simultaneous exchange of hydrogens through a transition state having two tricentric C-1–H–C-2 bonds. The production of D-[2-^{13}C,^{2}H]glucose from D-[1-^{13}C,^{2}H]mannose (Figure 2) confirms this exchange but shows that it is mediated solely by the C–C bond rearrangement. The H-1–C-1 and H-2–C-2 bonds are not broken, and no substantial deuterium isotope effect is seen in the reaction rate.

The fates of C-3 and H-3 were determined by reacting D-[1,3-^{13}C;3-^{2}H]mannose with molybdate. This reaction yielded only D-[2,3-^{13}C;3-^{2}H]glucose. It is clear that the rearrangement occurs without the loss of ^{2}H from C-3 and without C-3 transposition, eliminating mechanisms involving abstraction of H-3 with carbanion formation and subsequent nucleophilic attack at C-1.

Finally, as shown previously,[4] the reaction rates of D-mannose with molybdate in $^{2}H_2O$ and H_2O are similar, and no carbon-bound protons are exchanged.

Structural Requirements for the Reaction. Several analogues of mannose were treated under standard reaction conditions for 4 h to establish which functional groups are required for rearrangement. 3-Deoxy-D-[1-^{13}C]-*arabino*-hexose did not epimerize, although 6% reacted to produce a compound with a ^{13}C-enriched primary alcohol group resonating at 69.0 ppm. Bilik and Petrus[20] showed that 3-deoxy-D-*arabino*-hexose and 3-deoxy-D-*ribo*-hexose slowly form 3-deoxy-D-*erythro*-hexulose in an irreversible reaction, a result consistent with our observations. This result demonstrates that the formation of 2-keto isomers does not involve rearrangement of the carbon skeleton. More importantly, it demonstrates the absolute requirement of the C-3-hydroxyl group for C-2 epimerization.

4-Deoxy-D-*lyxo*-hexose yielded 14% of the C-2-epimeric 4-deoxy-D-*xylo*-hexose and 33% of other products after 4 h. In the same time, D-mannose would have reached equilibrium (Glc:Man = 72:28). It is evident that, while the 4-hydroxyl group is not essential for epimerization, its presence both increases the rate of reaction and limits the formation of other products.

Compounds that are unaffected by molybdate include mannitol, D-[1-^{13}C]glucosamine, 4,6-*O*-ethylidene-D-galactose, 4,6-*O*-ethylidene-D-glucose, 4-*O*-β-D-galactopyranosyl-D-[1-^{13}C]glucopyranose, and 4-deoxy-4-fluoro-D-[1-^{13}C]glucose. The last four compounds do not have a free hydroxyl group at C-4, and their failure to react demonstrates the importance of the 4-hydroxyl group in facilitating the reaction.

Mechanism of the Epimerization Reaction. The rearrangement reaction must involve a complex of molybdate with the reacting aldose. Both molybdate and the aldose can exist in a variety of forms in aqueous solution, and only one form of each may participate in the formation of the reactive complex. Molybdate forms isopolymeric species under the conditions used for the epimerization. At concentrations $>10^{-4}$ M and pH ≤ 5, molybdate is found principally as $Mo_7O_{24}^{6-}$ (paramolybdate).[21,22] Aldoses exist mainly as cyclic hemiacetals (pyranoses and furanoses), with aldehyde and hydrate forms generally present as a small percentage at equilibrium.

Many carbohydrates form complexes with molybdate.[23-26] Complexation with pyranose forms occurs most readily with compounds having an axial–equatorial–axial arrangement of hydroxyl groups (e.g., ribopyranose and talopyranose).[23] Most of these complexes have a 1:1 stoichiometry of molybdate:aldose. Weigel[24] has proposed that the molybdate is present as the oxo-bridged dimolybdate, $Mo_2O_5^{2-}$, with complexes taking the form [aldose–O_2Mo–O–MoO_2–aldose]$^{2-}$. However, these complexes cannot be important for molybdate-catalyzed epimerization since aldoses that are unable to form them, e.g., xylose and glucose, react faster (see below) than those that can. On the other hand, all linear polyols having four adjacent hydroxyl groups form stable dimolybdate complexes, (Mo_2O_5–polyol)$^{2-}$, making the linear aldehyde forms logical candidates for the reactive species.[25]

Support for involvement of the aldehyde is provided by the observations of Bilik et al.[5] that the reaction occurs up to 20 times slower at pH 5.9 than in the pH range 2.5–3.5. The rate of anomerization of aldoses has a similar pH dependence.[27] In addition, complexation of molybdate with cyclic aldoses is strongest at pH 5.9,[5] while complex formation with acyclic forms is strongest below pH 3.0.[5,25] These characteristics suggest that the aldehyde is the reactive species in the C-2 epimerization reaction.

In light of the above arguments, we propose that the aldehyde forms of aldoses form anionic complexes with dimolybdate in-

(18) Bilik, V. *Chem. Zvesti* **1972**, *26*, 183–186.
(19) Angyal, S. J. *Angew. Chem., Int. Ed. Engl.* **1969**, *8*, 157–166.
(20) Bilik, V.; Petrus, L. *Collect. Czech. Chem. Commun.* **1978**, *43*, 1159–1162.
(21) Schvarzenbach, G.; Meier, J. *J. Inorg. Nucl. Chem.* **1958**, *8*, 302–303.
(22) Kula, J. *Anal. Chem.* **1966**, *38*, 1382–1388.
(23) Bourne, E. J.; Hutson, D. H.; Weigel, H. *J. Chem. Soc.* **1960**, 4252–4256.
(24) Weigel, H. *Adv. Carbohydr. Chem.* **1963**, *18*, 61–77.
(25) Angus, H. J. F.; Bourne, E. J.; Weigel, H. *J. Chem. Soc.* **1965**, 21–26.
(26) Alfoldi, J.; Bilik, V.; Petrus, L. *Collect. Czech. Chem. Commun.* **1980**, *45*, 123–126.
(27) Isbell, H. S.; Pigman, W. W. *J. Res. Natl. Bur. Stand.* **1938**, *20*, 773–798.

Scheme I

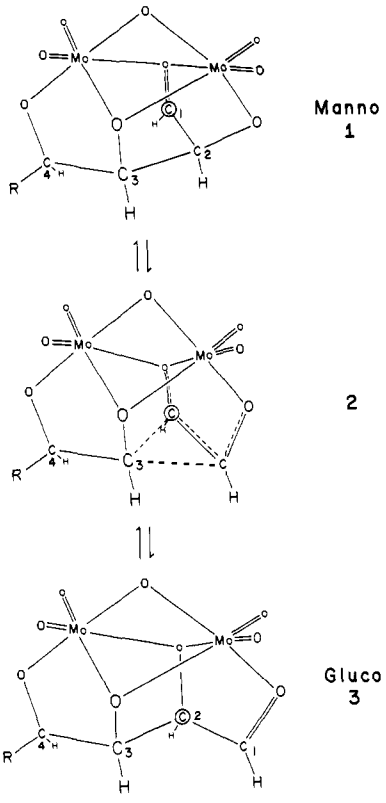

volving the carbonyl oxygen and the hydroxylic oxygens at C-2, C-3, and C-4 (**1**). In this complex, rearrangement (epimerization) can occur through a transition state (**2**) in which C-1 and C-2 are enantiomeric. Bond formation between C-2 and C-3 regenerates the starting aldose while bond formation between C-1 and C-3 produces the 2-epimer (**3**). Besides catalyzing bond breaking and formation, the molybdate complex assures the stereospecificity of the rearrangement. In the complex, only the 2-epimeric aldoses can form through inversion of the C-1–C-2 fragment. The configuration at C-3 is maintained since bond breaking and bond formation occur on the same face of this carbon. Formation of a strong complex with molybdate induces rehybridization so that in the transition state, C-1 and C-2 have the same hybridization and form a transitory tricentric bond with C-3.

This mechanism is consistent with all of the experimental observations: (a) only aldoses react, (b) OH-2 and OH-3 are essential, (c) OH-4 is not essential but is an important determinant of rate, (d) H-1, H-2, and H-3 are retained in the reaction, and, most importantly, (e) epimerization at C-2 is accompanied by a 1,2-shift in the carbon skeleton.

The participation of two molybdates in the productive complex is supported by observations that most polyols form such complexes below pH 6 involving four adjacent hydroxyl groups.[25] Of the five compounds studied that do not have a free hydroxyl group at C-4, only 4-deoxy-D-*lyxo*-hexose showed any reaction with molybdate. Space-filling molecular models of 4-deoxyaldoses show that OH-5 can be oriented to produce an arrangement of four oxygen atoms similar to that produced by O-1–O-4 in the aldoses. Molybdate complexes involving OH-5 are less favored than those involving OH-4, which may explain the slower reaction rates found for 4-deoxyaldoses.

The structures shown in Scheme I are based on those determined by X-ray crystallography for the mannitol[28] and D-lyxose[29] molybdate complexes. Other structures are possible, with O-1 and O-4 of the gluco isomer serving as the bridging oxygens instead of O-2 and O-3 as shown. This alternative complex would rearrange to form mannose with O-2 and O-4 serving as bridge

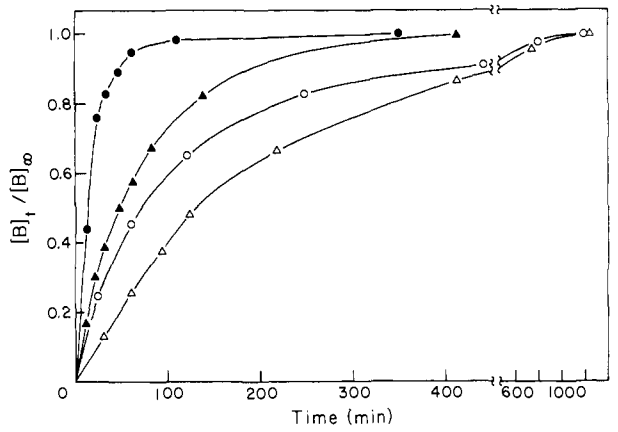

Figure 3. Comparison of the rates of molybdate-catalyzed epimerization of D-[1-^{13}C]aldoses. Samples containing the [1-^{13}C]aldose (0.1 M) and ammonium molybdate (0.01 M), pH 4.5, were incubated at 90 ± 1 °C in the NMR spectrometer and/or a circulating water bath at the same temperature. Spectra were taken at intervals. The concentration of the product [2-^{13}C]aldose at each time point ($[B]_t$) divided by its equilibrium concentration ($[B]_\infty$) is plotted vs. time: (●) glucose → mannose, (▲) mannose → glucose, (○) galactose → talose, (△) talose → galactose.

Scheme II

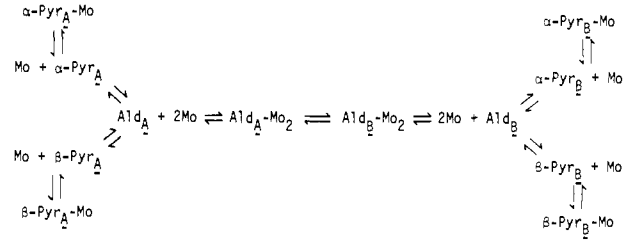

atoms. The examination of molecular models does not suggest which arrangement is preferred.

Kinetic Analysis. This study has confirmed the observations made by Bilik et al.[5] on the rates of epimerization of aldoses: rates increase with increasing temperature, increasing concentration of molybdate, and decreasing pH.

Kinetic studies are complicated by the presence of unreactive complexes involving cyclic forms, in addition to the reactive complexes involving the aldehyde form, as shown in Scheme II. This complexity is reflected in the reaction rates of pairs of C-2 epimeric aldoses. For example, under what appear to be similar conditions, the galactose to talose conversion reaches equilibrium faster than the talose to galactose conversion (Figure 3). For a simple reversible reaction (A ⇌ B), plots of $[B]_t/[B]_\infty$ vs. time examined for both directions should be coincident. The fact that they are not can be interpreted by considering that α- and β-talopyranoses form stable but unreactive tridentate molybdate complexes involving the axial–equatorial–axial arrangement of OH-2, OH-3, and OH-4.[23,26] This arrangement cannot be achieved in galactopyranoses. The formation of unreactive complexes causes the concentration of free molybdate in the reaction to be inversely proportional to the amount of talose present. Therefore, early in the talose to galactose conversion, the effective molybdate concentration is lower than its apparent concentration and the rate of reaction is slower than expected. In the conversion of galactose to talose, however, the effective molybdate concentration is high initially and the reaction procedes rapidly. These factors complicate the determination of rate constants.

For equilibrium reactions, the overall rate constant for the conversion of A to B must equal that for the conversion of B to A, since both are the sum of the intrinsic rate constants for the forward and reverse reactions ($k_f + k_r$).[30] As discussed above, this expectation is not fulfilled in the galactose–talose interconversion (Table II). That this anomaly is due to the formation

(28) Godfrey, J. E.; Waters, J. M. *Cryst. Struct. Commun.* **1975**, *4*, 5–8.
(29) Taylor, G. E.; Waters, J. M. *Tetrahedron Lett.* **1981**, *22*, 1277–1278.
(30) Frost, A. A.; Pearson, R. G. "Kinetics and Mechanism"; Wiley: New York, 1961; p 186.

Table II. First-Order Apparent Rate Constants for Epimerization of [1-^{13}C]Aldoses[a]

Gal → Tal			Tal → Gal		
t, min	$[B]_t/[B]_\infty$	10^3k, min^{-1}	t, min	$[B]_t/[B]_\infty$	10^3k, min^{-1}
26	0.25	11.0	32	0.13	4.3
61	0.45	9.9	62	0.25	5.0
122	0.65	8.6	94	0.37	5.0
248	0.83	7.2	219	0.67	5.3
441	0.91	5.5	413	0.89	5.5

[a] Starting aldose (0.1 M) was treated with molybdate (0.01 M), pH 4.5, at 90 °C. [B] is the concentration of the product aldose.

Table III. First-Order Apparent Rate Constants for Epimerization Measured at Equilibrium Using [1-^{13}C]Aldoses[a]

	Gal → Tal		Tal → Gal	
t, min	$[B]_t/[B]_\infty$	10^3k, min^{-1}	$[B]_t/[B]_\infty$	10^3k, min^{-1}
68	0.24	4.0	0.26	4.3
90	0.30	4.0	0.31	4.1
194	0.51	3.7	0.54	4.0
221	0.59	4.0	0.57	3.8
360	0.76	4.0	0.72	3.6

[a] An equilibrium mixture of 2-epimeric [1-^{13}C]aldoses (0.12 M Gal, 0.03 M Tal) was treated with molybdate (4 mM), pH 4.5, at 90 °C. [B] is the concentration of the product aldose.

of unreactive complexes is shown in an experiment that eliminates their effect on reaction rates. The rates of conversion of epimeric pairs can be measured simultaneously in mixtures of 1-^{13}C-enriched 2-epimeric aldoses, by using initial concentrations equal to those in the equilibrium mixture. In this approach, reaction conditions experienced by the two aldoses are identical and constant throughout the course of the reaction.

For example, an equilibrium mixture of galactose and talose (80:20) was prepared with 1-^{13}C-enriched compounds, molybdate was added, and the reaction mixture was incubated at 90 °C in the NMR spectrometer. Spectra were taken at intervals. The rates of conversion of galactose to talose and talose to galactose were followed simultaneously as, with time, [1-^{13}C]galactose converted to [2-^{13}C]talose and [1-^{13}C]talose converted to [2-^{13}C]galactose. The total concentration of each aldose, and, therefore, the concentration of free molybdate remained constant throughout the experiment. Rate constants obtained under these conditions (90 °C, MoO_3:aldose = 1:40) are essentially identical (Table III). Values of k_f and k_r can be obtained from these apparent rate constants and the measured equilibrium constant, $K_{eq} = k_f/k_r$. For the galactose to talose conversion, $k_f = 8.3 \times 10^{-4}$ min^{-1} and $k_r = 3.2 \times 10^{-3}$ min^{-1}.

Differences in the reaction rates between the glucose and mannose epimers (Figure 3) also can be explained by the presence of unreactive complexes. Rates measured at equilibrium (glucose:mannose = 72:28) were essentially identical, and the intrinsic rate constants are $k_f = 9.5 \times 10^{-3}$ min^{-1} and $k_r = 2.4 \times 10^{-2}$ min^{-1}.

Configurational differences at sites other than C-2 also affect reaction rates. When measured under similar equilibrium reaction conditions, the rate of the glucose–mannose interconversion is approximately eight times faster than that of the galactose–talose interconversion (Figure 3). The difference is probably due in part to a higher effective molybdate concentration in the glucose–mannose case. However, the effect also could arise from steric interaction in the reactive complex (Scheme I). When either glucose or mannose binds with molybdate, the uncomplexed C-5–C-6 moiety extends away from the reaction site. In complexes involving galactose or talose, this moiety is gauche to C-2, with C-2, C-3, C-4, and C-5 having a sickle conformation. Complex formation in the latter case is hindered, causing slower reaction rates. The situation can be visualized by exchanging R with H at C-4 in **1**, **2**, and **3** (Scheme I). Similar effects would occur in the alternative complexes where O-4 is a bridge atom as discussed above.

Table IV. Secondary Product Formation in Aqueous vs. Aprotic Conditions

aldose	conditions[a]	% starting aldose	% C-2 epimer	% C-3 epimer	% C-2,3 epimer
[1-^{13}C]Tal	H_2O, 13 h	51	44	3	2
[1-^{13}C]Ara	H_2O, 4 h	55	26	7	12
[1-^{13}C]Ara	DMF, 24 h	67	28	1	4
[1-^{13}C]Xyl	H_2O, 13 h	36	22	26	16
[1-^{13}C]Xyl	DMF, 24 h	59	38	2	1
[2-^{13}C,^{2}H]Xyl	H_2O, 13 h	63	36	0	1

[a] Aqueous conditions: 0.1 M aldose, 0.01 M molybdate, pH 4.5, 90 °C. Aprotic conditions: 0.5 M aldose, 0.03 M $MoO_2(acac)_2$, 50 °C.

Scheme III

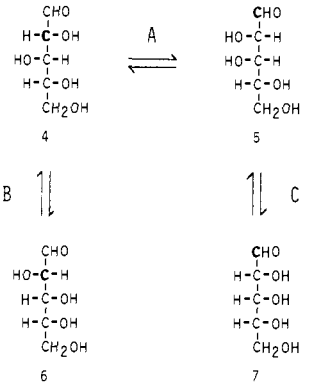

Secondary Reactions. When long reaction times or otherwise forcing conditions are used, secondary products are formed (Table IV). For example, in the galactose–talose interconversion, small amounts of gulose and idose are produced. When D-[1-^{13}C]talose is the starting aldose, the byproducts are D-[1-^{13}C]gulose and D-[2-^{13}C]idose. Bilik proposed that secondary products form by the simultaneous inversion of trans hydroxyl groups in pyranosyl sugars caused by the simultaneous exchange of hydrogen atoms at C-2 and C-3 in an aldopyranose–molybdate complex.[3]

The interconversions that could occur are shown in Scheme III, with D-[2-^{13}C,^{2}H]xylose (**4**) as an example. There are three different reactions. The first (A) is the rearrangement of the C-1–C-2 fragment. The second (B) can only occur when OH-2 and OH-3 are trans and involves the exchange of H-2 and H-3 with inversion of configuration at C-2 and C-3. The third (C) involves the simultaneous inversion of cis hydroxyls at C-2 and C-3.

Bilik and Petrus[31] presented evidence that reactions of type B occur in stable ring systems such as 1,5-anhydro-6-deoxy-L-galactitol. The mechanism was proposed, however, on the basis that H-1 and H-2 appear to exchange in reactions of type A in aldoses. In this study we have demonstrated that the apparent exchange of hydrogens in reaction A is caused by the C-1–C-2 transposition. Nevertheless, the vicinal proton exchange mechanism proposed by Bilik et al.[4] may operate in reaction B. Evidence supporting this mechanism was obtained from the reaction of D-[2-^{13}C,^{2}H]xylose (**4**) with molybdate. Pentoses with ^{1}H at C-2 readily undergo both reactions A and B to give an equilibrium mixture of all four pentoses.[3] Unlike D-xylose or D-[2-^{13}C]xylose, the 2-^{2}H compound under similar reaction conditions gives rise to D-[1-^{13}C,^{2}H]lyxose (**5**) only. By analogy to reactions involving proton abstraction or hydride shifts, a substantial deuterium isotope effect is expected for the transfer of hydrogens; the substitution of ^{2}H for ^{1}H at C-2 should substantially reduce the rate of reaction involving transfer of H-2.

In the rearrangement of **4**, neither arabinose (**6**) nor ribose (**7**) is formed. While the formation of arabinose is inhibited by the presence of ^{2}H at C-2, the formation of D-[1-^{13}C,^{2}H]ribose (**7**)

(31) Bilik, V.; Petrus, L. *Chem. Zvesti* **1979**, *33*, 114–117.

by reaction C would not be inhibited. The failure of ribose to form suggests that reaction C, if it occurs, is very slow relative to reactions A and B.

The formation of secondary products is substantially reduced when the dioxobis(2,4-pentanedionato-*O,O'*)molybdenum(VI) complex is used and DMF is the solvent.[16] This is the preferred method for the interconversion of pentoses and tetroses (Table IV).

Trioses and Tetroses. DL-[1-^{13}C]Glyceraldehyde gives only small amounts of DL-[2-^{13}C]glyceraldehyde when incubated with molybdate; [1-^{13}C]dihydroxypropanone is the major product.[32]

D-[1-^{13}C]Threose in aqueous molybdate rearranges rapidly to give D-[2-^{13}C]erythrose and other products (16%) that were not identified. The reaction gives only the expected 1,2 inversion in DMF. The facile rearrangement of tetroses and the limited reaction of glyceraldehyde provide further evidence of the importance of four aldose oxygens in the formation of the reactive molybdate–sugar complex.

Summary

The C-2 epimerization of aldoses catalyzed by molybdate occurs with exchange of C-1 and C-2 by inversion of the C-1–C-2 aldol fragment. The nature of the skeletal rearrangement and an examination of the reactivity of analogues of aldoses suggest that the reactive complex involves two molybdate moieties and four oxygens of the aldehyde form of the aldose. Structural features that interfere with complex formation inhibit the reaction. Rates of conversion are strongly influenced by the formation of stable and unreactive molybdate complexes with ring forms of the aldoses. Secondary reactions that involve the simultaneous inversion of configuration of adjacent trans hydroxyl groups occur more slowly and by a different mechanism.

Acknowledgment. This work was supported in part by Grant GM-21731 from the Institute of General Medical Sciences, National Institutes of Health, Bethesda, MD. We thank Dr. James R. Rasmussen for his generous gift of deoxy and fluoro aldoses.

Registry No. $MoO_2(acac)_2$, 17524-05-9; molybdic acid, 11099-00-6; D-[1-^{13}C]mannose, 70849-16-0; D-[2-^{13}C]glucose, 70849-17-1; D-[1-^{13}C]talose, 70849-29-5; D-[1-^{13}C]galactose, 70849-30-8; D-[1-^{13}C]glucose, 40762-22-9; 6-deoxy-L-[1-^{13}C]talose, 83379-33-3; 6-deoxy-L-[2-^{13}C]-talose, 83379-34-4; D-[1-^{13}C]xylose, 70849-21-7; D-[1-^{13}C]arabinose, 70849-23-9; D-[2-^{13}C]galactose, 83379-35-5; D-[2-^{13}C]talose, 83379-36-6; D-[2-^{13}C]mannose, 70849-16-0; L-[2-^{13}C]fucose, 83379-37-7; L-[1-^{13}C]-fucose, 83379-38-8; D-[2-^{13}C]xylose, 83379-39-9; D-[2-^{13}C]ribose, 83379-40-2; 3-deoxy-D-[1-^{13}C]-*arabino*-hexose, 83379-41-3; 4-deoxy-D-*lyxo*-hexose, 74164-24-2; 4-deoxy-D-*xylo*-hexose, 7286-46-6; mannitol, 69-65-8; D-[1-^{13}C]glucosamine, 83379-42-4; 4,6-*O*-ethylidene-D-galactose, 6207-17-6; 4,6-*O*-ethylidene-D-glucose, 13403-24-2; 4-*O*-β-D-galactopyranosyl-D-[1-^{13}C]glucopyranose, 83379-43-5; 4-deoxy-4-fluoro-D-[1-^{13}C]glucose, 83379-44-6; D-[1-^{13}C]threose, 70849-20-6; D-[2-^{13}C]erythrose, 83434-88-2; D-[1-^{13}C,^{2}H]mannose, 83379-45-7; D-[2-^{13}C,^{2}H]glucose, 83379-46-8; ammonium molybdate, 11098-84-3.

(32) Konigstein, J. *Collect. Czech. Chem. Commun.* **1978**, *43*, 1152–1158.

Mechanism of the Aminolysis of Alkyl Benzimidates[1]

Hiram F. Gilbert[2] and William P. Jencks*

Contribution No. 1429 from the Graduate Department of Biochemistry, Brandeis University, Waltham, Massachusetts 02254. Received March 26, 1982

Abstract: The aminolysis of a series of ring- and alkyl-substituted benzimidates proceeds through a mechanism involving the formation and decomposition of a tetrahedral intermediate as evidenced by a change in rate-determining step with changing pH. On the alkaline side of the pH–rate profile, formation of the tetrahedral intermediate from the free amine and protonated benzimidate is rate determining. Structure reactivity correlations for this step show a late (intermediate-like) transition state with $\beta_{nuc} = 0.61$, $\beta_0 = -0.47$ (for O-substituted benzimidates), and $\rho = 1.49$. There is no evidence for a kinetically significant proton-transfer step. The addition of water to alkyl benzimidates follows $\beta_0 = -0.56$. On the acidic side of the pH–rate profile for aminolysis, the breakdown of the intermediate with expulsion of alcohol is the rate-determining step, as evidenced by the observation of an exchange reaction of methoxyamine for ammonia. The neutral tetrahedral intermediate (T_0) partitions between acid-catalyzed expulsion of alcohol, ammonia, and methoxyamine with partition ratios of approximately 1/1/300, respectively. The expulsion of alcohol also occurs by a spontaneous (water catalyzed) reaction characterized by $\beta_0 = -1.30$ and $\rho = -0.01$, suggesting a late (product-like) transition state for this reaction. The expulsion of alcohol through a general-acid-catalyzed reaction is characterized by relatively low Brønsted α values of 0.40–0.49. The decrease in α with decreasing pK of the leaving alcohol can be described by an interaction coefficient $p_{xy} = 1/c_5 = \delta\alpha/\delta pK_{lg} = 0.05$. This reaction can be described on a structure–reactivity diagram by a diagonal reaction coordinate that represents concerted proton transfer and C–O bond cleavage in the transition state. The effect of structure on the direction of acid-catalyzed expulsion of alcohols and amines from addition compounds is reviewed briefly.

Most imine-forming elimination reactions[3-11] consist of the following types:

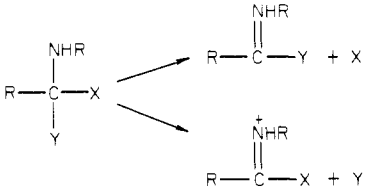

(1)

in which X and Y are R, OR, or NHR. In order to provide a more complete picture of these reactions, we have studied the

(1) Supported by grants from the National Institutes of Health (GM-20888) and National Science Foundation (PCM77-08369). Dr. Gilbert was supported by an American Cancer Society fellowship (PF-1111).

(2) Present address: Department of Biochemistry, Baylor College of Medicine, Houston, TX 77030.

(3) Sayer, J. M.; Peskin, M.; Jencks, W. P. *J. Am. Chem. Soc.* **1973**, *95*, 4277–4287.
(4) Sayer, J. M.; Jencks, W. P. *J. Am. Chem. Soc.* **1977**, *99*, 464–474.
(5) Gravitz, N.; Jencks, W. P. *J. Am. Chem. Soc.* **1974**, *96*, 489–499, 499–506.
(6) Gravitz, N.; Jencks, W. P. *J. Am. Chem. Soc.* **1974**, *96*, 507–515.
(7) Hogg, J. L.; Jencks, D. A.; Jencks, W. P. *J. Am. Chem. Soc.* **1977**, *99*, 4772–4778.
(8) Fischer, H.; DeCandis, F. X.; Ogden, S. D.; Jencks, W. P. *J. Am. Chem. Soc.* **1980**, *102*, 1340–1347.
(9) Burdick, B. A.; Benkovic, P. A.; Benkovic, S. J. *J. Am. Chem. Soc.* **1977**, *99*, 5716–5725.

0002-7863/82/1504-6769$01.25/0